

Global evaluation of economics of microalgae-based biofuel supply chain using GIS-based framework

Seongwhan Kang^{*}, Matthew J. Realf^{**}, Yanhui Yuan^{***}, Ronald Chance^{**,**}, and Jay Hyung Lee^{****,†}

^{*}R&D Campus Daejeon, LG Energy Solution, 188 Munji-ro, Yuseong-gu, Daejeon 34122, Korea

^{**}School of Chemical and Biomolecular Engineering, Georgia Institute of Technology, 311 Ferst Drive, NW, Atlanta, GA 30332, USA

^{***}Algenol Biotech, 16121 Lee Road, Fort Myers, FL 33912, USA

^{****}Department of Chemical and Biomolecular Engineering, Korea Advanced Institute of Science and Technology (KAIST), 291 Daehak-ro, Yuseong-gu, Daejeon 34141, Korea

(Received 27 August 2021 • Revised 14 December 2021 • Accepted 22 December 2021)

Abstract—A microalgae-based biofuel supply chain was designed for different geographic regions, considering the local environmental conditions of sunlight, temperature, and available resources of water and CO₂. The supply chain was designed in three distinct areas, Texas, U.S., Northern Territory of Australia, and La Guajira, Colombia, selected through a global analysis of suitable land based on GIS. A three-stage design framework developed in our previous research was improved to include a biomass productivity estimation model based on operating data provided by Algenol, a new photobioreactor (PBR) cultivation technology, direct air capture of CO₂ as a feedstock option, and functional-unit based optimization. The framework focuses on the comparison of two major cultivation platforms, open raceway pond (ORP) and photobioreactor (PBR) using a net present value metric. A mixed-integer fractional programming (MIFP) model was formulated to make multi-period strategic and tactical decisions related to the supply chain design and operation under the objective of minimizing the total cost per gasoline gallon equivalent of products (GGE). Under the same assumptions, the supply chain was designed for seven years and the cost was estimated to be \$15.5, \$13.5, and \$14.0/GGE for the U.S., Colombia, and Australia, respectively. While various processing pathways were considered in the model, only a single pathway involving PBR, an algae strain AB1166, and hydrothermal liquefaction was selected in all regions owing to its cost-efficiency. Direct air capture and hypothetical saline water species scenarios were examined to analyze the effect of alternative resource sources on the supply chain design and economics.

Keywords: Microalgae-based Biofuel, Supply Chain Design, Geographic Information System (GIS), Global Evaluation, Mixed Integer Fractional Programming (MIFP), Direct Air Capture

INTRODUCTION

The adverse environmental impact of increased atmospheric CO₂ concentration caused by the use of fossil energy has led to a heightened interest in the development of biofuels with lower carbon footprint. Biofuels could play an important role in the 'hard-to-defossilize' transportation sector with a product that allows the use of current fuel distribution infrastructure and internal combustion engines [1]. Therefore, various regulatory and legislative initiatives have been proposed in many countries and by international organizations to expedite the production of biofuels. Under the International Energy Agency's Sustainable Development Scenario, the amount of global transport biofuel consumption is targeted to be 298 Mtoe by 2030, which is almost triple the production amount of 2019 [2]. However, the steeply increasing demand for biofuel will eventually lead to first-generation crop-based biofuels competing with food production and limiting their contribution to the development of sustainable energy systems [3]. Such issues have

brought the transition of targets in biofuel feedstock development from crop-based biomass to non-food biomass. The development of microalgae-based biofuels has been advocated due to their high areal productivity and ability to be sited on land unsuitable for conventional food crops. Moreover, algal biofuels have been reported to show the lowest emissions and best engine performance compared with crop and waste cooking oil-oriented biofuels [4]. Despite their high potential, the commercialization of microalgae-based biofuels is lacking since the estimated production cost is still higher than the target of \$3 per gallon of gasoline-equivalent (GGE) suggested by the U.S. Department of Energy (DOE) [5].

Effective cost reduction requires careful process cost analyses to determine which subsystems contribute to the cost the most and how they can be improved. For this purpose, techno-economic analysis (TEA) studies have been performed under various assumptions and scenarios regarding the factors that affect the production costs of microalgae-based biofuel [6]. However, most studies have not considered the geographical factors that could affect the economics and feasibility of microalgae-based biofuels. The geographical factors related to the economics and feasibility of biofuels can be classified as weather conditions, land availability, and resource availability. Weather conditions, such as irradiance level and ambient

[†]To whom correspondence should be addressed.

E-mail: jayhlee@kaist.ac.kr

Copyright by The Korean Institute of Chemical Engineers.

temperature, can strongly influence microalgae areal productivity, resulting in significant variability in the production cost. Banerjee et al. showed the variation in productivity and economics of microalgae biomass in different geographical locations in the U.S. using mathematical modeling and economic analysis [7]. The cost varied between \$500/ton and \$9560/ton depending on the location and cultivation technology selected. Furthermore, large-scale microalgae cultivation requires a certain extent of flat and barren land areas and a substantial amount of water and nutrients such as CO₂, nitrogen, and phosphorous. Therefore, these land and resource constraints restrict microalgae-based biorefineries only to locations with suitable conjunction of available land, resources, and climate and incur additional costs of resource transportation when these are not co-located. Correa et al. performed a global land suitability evaluation of microalgae-based biofuel under some economic and environmental criteria to screen the most suited land for microalgae-based biofuel production [8]. The analysis found 132,900 km² to 1,422,800 km² suitable areas according to the water and CO₂ supply scenarios selected, which is 0.09% to 0.96% of the global land area. Thus, to consider these effects and constraints caused by geographic factors efficiently, the research scope should be switched from a single biorefinery to a supply chain that manages not only the biofuel production with multiple biorefineries but also the feedstock procurement and product distribution.

To address this knowledge gap, several studies have been conducted on the development of a microalgae-based biofuel supply chain by integrating mathematical optimization with the geographic information system (GIS). Nodooshan et al. designed a multi-objective microalgae-based biodiesel supply chain in the Midwest region in the U.S. for seven-year periods [9]. The GIS was utilized to screen candidate locations for the biorefinery according to the land cover data and to obtain location information and resource availability of resource suppliers. The model was solved under the minimization of total costs and greenhouse gas emissions and resulted in Pareto-optimal solutions that included different individual supply chain designs. Kang et al. designed the high spatial resolution supply chain by developing a three-stage framework that integrates biorefinery design, GIS analysis, and mathematical optimization [10]. The GIS analysis included a candidate location screening process utilizing various land and resource constraints. A case study was performed for Texas, U.S., for ten-year periods considering seasonal variations of parameters, and scenario studies were performed to reduce production costs. Mohseni et al. performed the supply chain design in an Iranian territory by considering uncertainty in the process parameters by a robust optimization approach [11]. To find the candidate locations for the biorefinery in Iran, an analytical hierarchy process was integrated with GIS to score the suitability index of land areas with selected weather, land, and resource criteria.

Despite these previous research efforts, the design model for the biofuel supply chain can be improved further by addressing several gaps. First, all case studies published to date considered a single geographic area. Since geographical features vary widely with location, differences in the design and production costs among diverse areas should be analyzed to capture their effects. For instance, closer to the equator, biomass productivity fluctuation between seasons de-

creases, and the annual average productivity increases, because of the inherent reduction in the variation and increase in the number of hours of sunlight. This leads to a reduction in production cost since the absolute value and variation of biomass productivity have high impacts on the costs as detailed in our previous supply chain design study [10]. Furthermore, not only the biomass productivity but also the land and resource availability of each location will affect the feasibility and economics of the biofuel. Therefore, case studies conducted in multiple geographic regions will give important insights into how these factors affect supply chain design and production costs. The cultivation infrastructure is the most expensive component of the microalgae-based biorefinery since its processing scale is the largest among the processing stages and the biomass productivity directly impacts costs associated with downstream processing systems [12]. Therefore, the process design of the cultivation stage including the selection of microalgae species and cultivation technology greatly influences the overall production costs. Moreover, process designs are also related to geographical features such as land and resource availability. For example, since photobioreactors (PBRs) yield much higher areal productivity and lower CO₂ leakage than open raceway ponds (ORPs), a PBR-based biorefinery requires less land area and CO₂ supply for the same amount of biomass production. Thus, designing the supply chain for an area that has low land availability and CO₂ supply, PBRs may be preferred to ORPs despite their higher capital and operating costs. Therefore, the cultivation process design must be a part of the supply chain design model to find the best cultivation strategy for optimized economics of microalgae-based biofuel. However, to the best of our knowledge, only one study [10] has considered the effect of microalgae species in the model and none of the studies have considered cultivation technology as a decision variable in the optimal design.

This paper presents a microalgae-based biofuel supply chain design formulation for different global areas to compare the supply chain configurations and production costs of biofuel and investigate the effects of geographical factors. The case study areas were selected via a global analysis of suitable lands based on land availability and biomass productivity. After selecting the suitable areas, the three-stage design framework developed in our previous study was applied to design the best possible supply chain in each chosen area [10]. Since our previous design framework only considered the selection of microalgae species among the cultivation process design requisites, the model was modified to consider the selection of cultivation technology options. The process data and biomass productivity model developed by Algenol were applied in the framework for comparison under the same basis [13,14]. Algenol has developed a microalgae-based biofuel with two pathways to biofuel: ethanol production from genetically modified cyanobacteria and biocrude production from microalgae biomass. The data used herein were generated from its pilot-scale plant operations in Florida and India. In addition, the productivity model used was validated at both laboratory and pilot scales for both ethanol and biocrude production. While many research studies have used approaches based on hypothetical target values or lab-scale values for biomass productivity and process parameters, the application of the validated, pilot-scale data enhances the reliability of the projected results. The mathemati-

cal optimization was formulated as a mixed-integer fractional programming (MIFP) problem to minimize total supply chain costs per GGE (gallon gasoline equivalent) of products in order to identify the present state of the economics of microalgae-based biofuel and in relation to the \$3/GGE target set by the Department of Energy. However, the nonconvexity and a large number of location inputs cause difficulties in solving the optimization problem directly using a conventional MINLP solver. Moreover, the local MINLP solver cannot guarantee the global optimality of the solution obtained. Therefore, the inexact parametric algorithm based on Newton's method, which is a tailored global optimization algorithm for solving large-scale and non-convex MIFP problems was used to solve the problem efficiently [15]. After the base case designs were established for each region, alternative resource supply strategies, e.g., CO₂ direct air capture (DAC) and hypothetical saline water species, were applied, respectively, to identify the effect of scenarios on the supply chain design and economics.

As a summary, major novelties and contributions of the present work are listed below.

- The microalgae-based biofuel supply chains are designed in multiple regions by a systematic approach integrated with GIS and mathematical optimization to analyze the effect of geographical features on the designs and economics of the supply chain.
- In the process design, microalgae species and processing technology are considered as decision variables in the model to find the best biomass production strategy in each area.
- Multiple fuel products are considered in the supply chain design

for an optimal fuel product selection according to the GGE-based analysis.

- The minimization of the total cost per GGE is used as the objective function to estimate the economics in each region. Due to the complex nature of the formulated MIFP, a tailored global optimization algorithm is used.
- CO₂ direct air capture (DAC) is included as an option to supplement any local CO₂ supply from industrial sources. Importance of doing so is demonstrated.

The paper is organized as follows. The microalgae-based biofuel supply chain system is described in Section 2. The methods used for the screening of case study regions and supply chain design options are explained in detail in Section 3. The results of the global analysis of suitable land and supply chain designed in each case study region are presented in Section 4. Finally, in Section 5, scenario studies are conducted to investigate the transition of supply chain design and economics under the alternative resource supply methods - direct air capture for CO₂ and hypothetical saline water species for water.

PROBLEM DEFINITION

As stated in the Introduction, the objective of the supply chain design model is to enable the search for the best supply chain configuration under a cost per GGE minimization objective function in each geographic region considered. Thus, the model should include basic structural elements of the supply chain and represent

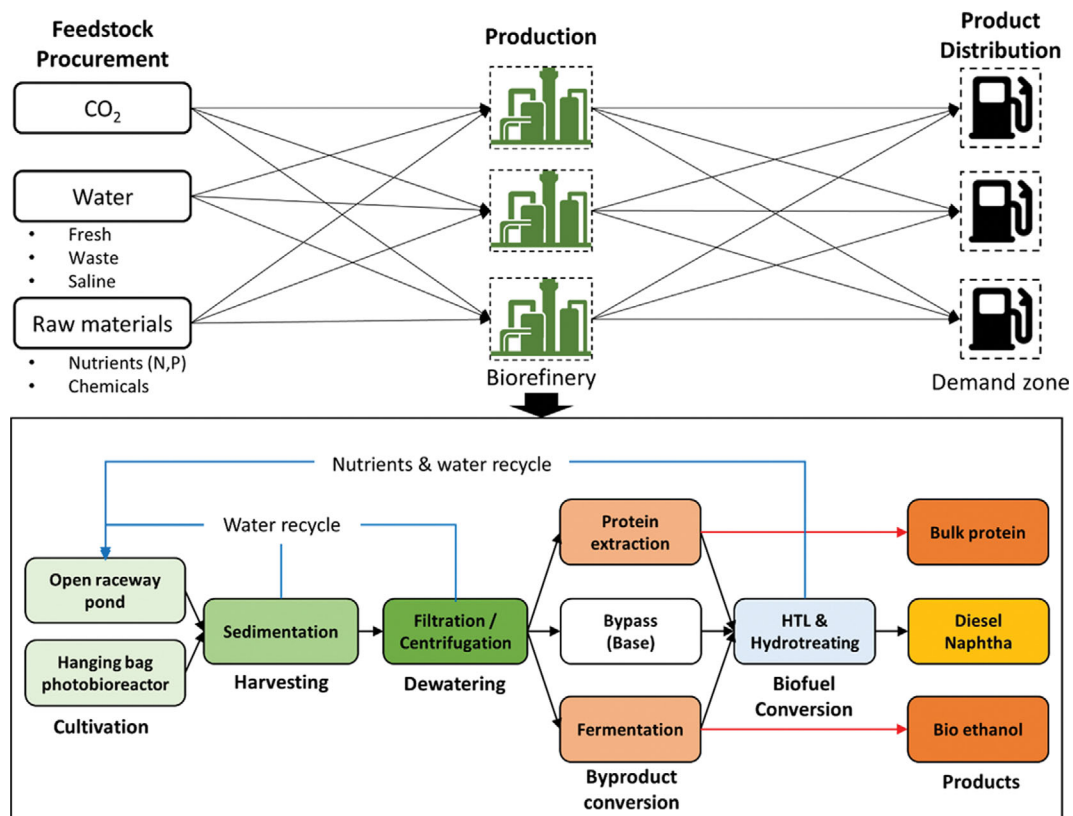


Fig. 1. The overall structure of the microalgae-based biofuel supply chain with detailed processing pathways of a biorefinery.

decisions to be made for each constituent of the structure. The main structure of a microalgae-based supply chain and processing pathways of a biorefinery is depicted in Fig. 1. The supply chain comprises three stages: feedstock procurement, production, and product distribution. First, feedstocks required for a biorefinery such as CO₂, water, and nutrients are supplied from each source via appropriate transportation methods, e.g., pipelines and trucking. Then, biofuel and byproducts are produced using the supplied feedstock in microalgae-based biorefineries. The biorefinery consists of sequential processing stages from the microalgae cultivation to the biofuel conversion that produces the main product, the microalgae-based biofuel. As shown in the lower part of Fig. 1, the microalgae-based biorefinery designed in this study has multiple processing pathway options according to the selection of microalgae species, cultivation, and byproduct conversion technology. Each processing pathway results in different products and processing costs. Finally, the products are transported to demand zones, such as populated cities or ports for further distribution. The detailed description and assumptions of each stage are retained from our previous study [10].

The objective of the model is to make both strategic and tactical decisions in each project unit time. The strategic decisions are related to supply chain configurations, including the locations of elements of each supply chain stage and design of the biorefineries, while the tactical decisions include the material flows between the elements and the amounts of production. The design is selected using a multi-period formulation to handle the seasonal variation of the process parameters, such as the biomass productivity and

evaporation rate. Furthermore, since the demand for biofuel is expected to increase as discussed in the introduction section, the design should be expanded over time. Therefore, the project time unit is set as three months to consider the seasonal variation of the parameters, and the project period is set as seven years to investigate the effect of increasing demands. The detailed assumptions of each element in the supply chain are discussed and referred from the previous supply chain design study [10].

METHODOLOGY

The overall research methodology is depicted in Fig. 2. First, the case study regions are identified by a global scan for suitable land. The suitable lands are identified by utilizing the available lands and biomass productivity screening criteria. According to the result of the screening, case study regions are selected which have different geographic characteristics to compare their effects on the configurations and economics of microalgae-based biofuel supply chains. Then, the supply chain is designed in each case study region using the three-stage framework developed in the previous work [10], but with the new global optimization formulation for the fractional program. Finally, the designed supply chain configurations and economics are compared between the regions. In this section, the details of the methodology are discussed.

1. Global Suitable Land Evaluation

Microalgae are a promising future biofuel feedstock because they do not need fertile land for cultivation and have higher areal productivity compared to first- and second-generation feedstocks. These

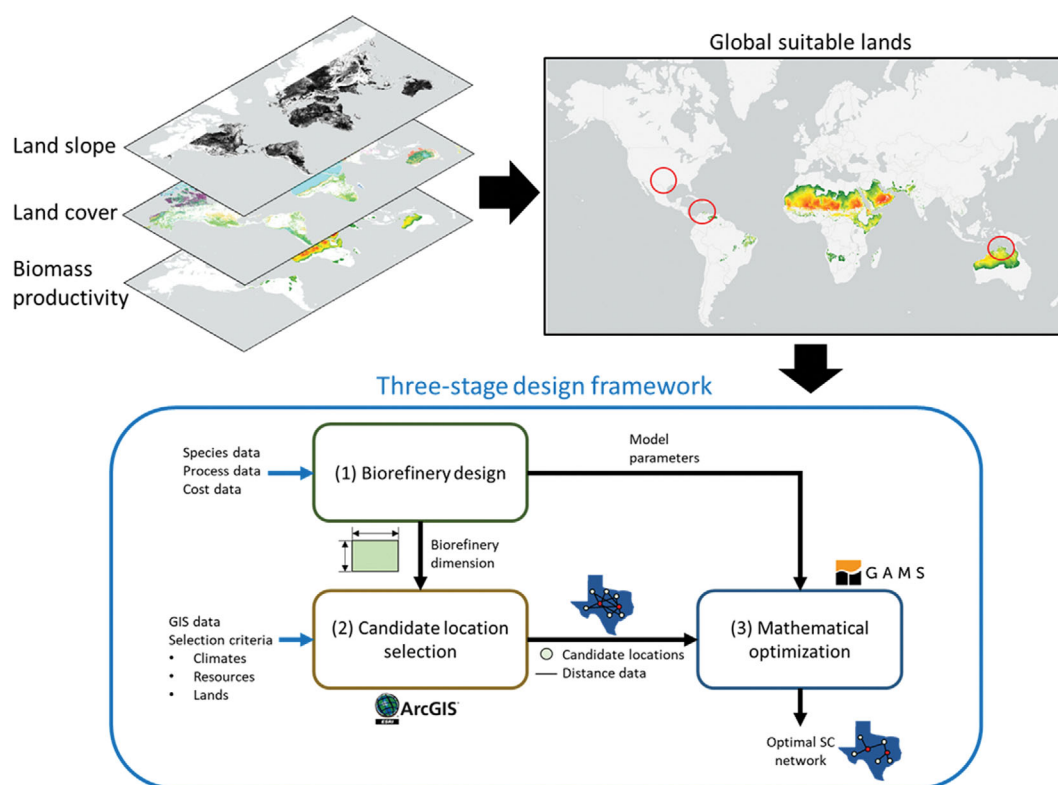


Fig. 2. Schematic diagram of the overall research methodology.

advantages lead to reduced competition with agriculture and for land that can support high biodiversity [8]. Moreover, an ORP frequently used for large-scale microalgal biomass production requires flat land to avoid significant construction and water pumping costs. Even for PBR deployment, flat land is a significant advantage. Given the high cost of microalgal cultivation infrastructure, locating places with high productivity and flat topography is an important first step.

Therefore, the commercial GIS software of ArcGIS Pro is used with land usage, land slope, and microalgae productivity as the basic screening criteria to obtain suitable lands for microalgae-based biorefinery. First, 300 m-resolution global land cover data from European Space Agency Climate Change Initiative (ESA-CCI) is used to screen out the infeasible and unsustainable lands such as urban areas, croplands, and water bodies [16]. The land cover data comprise 38 categories and among them, only barren, shrub, herbaceous, and grasslands are screened as feasible land since food production competition and other similar land usage issues need to be avoided. Then, the land slope is calculated using Shuttle Radar Topography Mission (SRTM) 90 m-resolution digital elevation map (DEM) provided by CGIAR-CSI [17]. Since the resolution of the two data layers is different, the land slope layer is resampled to a 300 m-resolution. Then, flat lands are screened by applying the slope restriction - less than 5%, which is the suggested slope restriction by the DOE algae road map [18]. The lands satisfying these two constraints are defined as available lands for microalgae-based biorefinery.

Not only land availability but also high biomass productivity is required for the economic feasibility of the biorefinery. Therefore, global biomass productivity with a PBR-based cultivation system is estimated using the productivity model developed by Algenol for this purpose [13,14]. The global $0.5^{\circ} \times 0.5^{\circ}$ grid point data of monthly average air temperature and sunlight intensity extracted from the NASA POWER database are used as inputs for the estimation model [19]. At each grid point, the annual average biomass productivity is calculated and interpolated to obtain the productivity map covering the entire world. Using the productivity map, we defined an area that has over $30 \text{ g/m}^2/\text{day}$ productivity as the high productivity area. This compares favorably to the $25 \text{ g/m}^2/\text{day}$ annual average obtained by Algenol (model and experiment) for Fort Myers, Florida. By combining the high productivity area and available land, we can obtain land areas suitable for microalgae-based biofuel production as shown in the upper right part of Fig. 2.

2. Three-stage Framework

A three-stage framework is developed to design a microalgae-based biofuel supply chain with a high spatial resolution by integrating the geographic information system (GIS) and mathematical optimization. The basic structure and description of the framework can be found in the previous work [10]. In this study, the previous framework is enhanced by:

- Considering photobioreactors as the preferred cultivation technology alternative
- Applying the economic and process parameters extracted from the pilot-scale microalgae cultivation facility operated by Algenol
- Estimating the microalgal biomass productivity based on the weather data to compare the effects of regional productivity differences

- Designing pipeline routes and size according to the geographical features and flow rates of resources
- Modifying optimization problem formulation to MIFP to find the best design under cost per GGE minimization

Therefore, the following sections will focus on these modifications of the framework.

2-1. Biorefinery Design

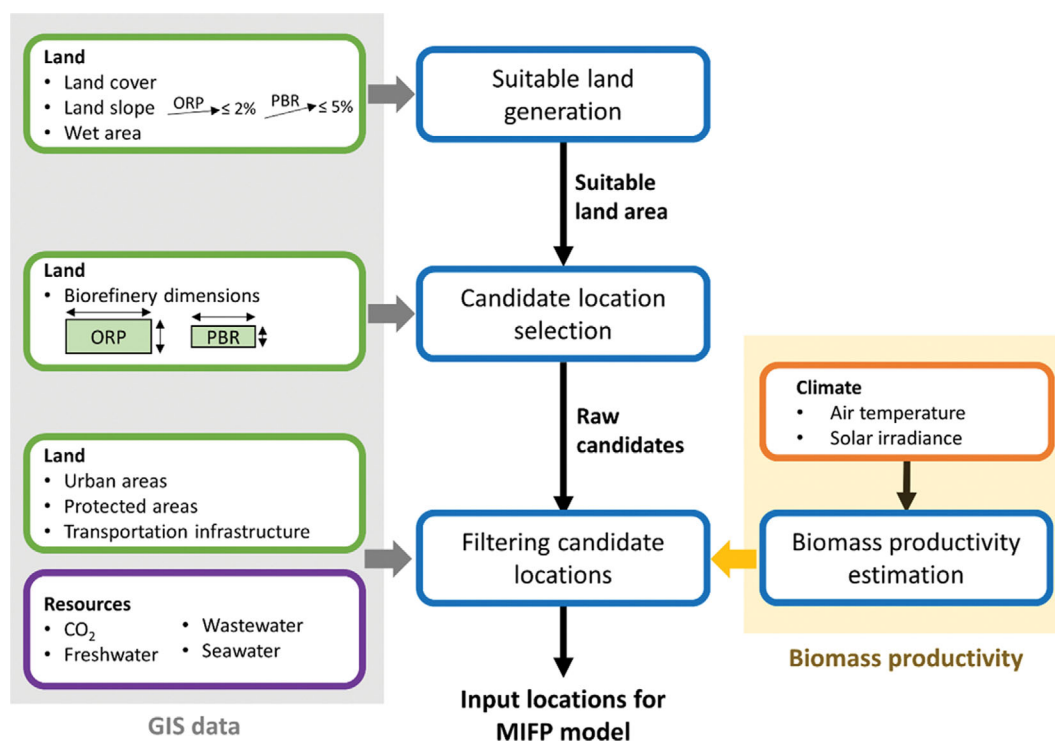
The proposed processing pathways of the biorefinery are shown in the lower part of Fig. 1. The biorefinery is composed of five sequential processing stages: microalgae cultivation, biomass harvesting, dewatering, byproduct conversion, and biofuel conversion. The processing pathway of the biorefinery is chosen depending on the selection of cultivation and byproduct technologies. Moreover, not only the processing pathway but also the selected microalgae species affect the output and the economics of the biorefinery. Therefore, TEAs are performed using a spreadsheet-based model modified from the previous study for each combination of the species and processing pathways. In this study, two microalgae species and six processing pathways are suggested as design options and they result in 12 possible design combinations. The process and economic parameters of the biorefinery are found from the biorefinery design calculations performed by Algenol [13]. While multiple capacities of an ORP-based biorefinery were considered in the previous study, only the maximum capacity, 6000 acre cultivation is considered here since the benefit of economics of scale overwhelms the transportation cost increase [10].

As mentioned in the Introduction, a closed PBR system is considered as the cultivation technology in the model. Among the various available designs of PBR, we applied the hanging bag PBR, named VIPER 3.4, which is a target cultivation technology developed by Algenol [13]. The main differences between ORP and PBR considered in this study are biorefinery layouts, processing costs, CO_2 utilization efficiency, water evaporation, and areal biomass productivity. These differences are summarized in Table 1. The layouts and dimensions of an ORP based facility and a PBR-based facility are modified from the design suggested in the NREL report [20]. The PBR facility is designed to have the same total biomass productivity as the ORP facility, and since a PBR is known to have about 3.0 times higher areal productivity than an ORP, the PBR facility has 2000 acres of cultivation area and 3915 acres of total facility size. Comparing the processing costs, a PBR facility has lower OPEX but higher CAPEX compared to an ORP facility. Since VIPER 3.4 is made of polyethylene-based film, equipment costs are lower than many other PBR options, but still significantly higher compared to ORPs. Meanwhile, PBRs need to be replaced more frequently compared to an ORP, which adds to a higher OPEX [13, 20]. On the other hand, PBR is superior to ORP in the aspect of water loss and CO_2 utilization efficiency because of its closed environment, and significantly more productive as already noted.

Another design option in the cultivation stage is the microalgae species. Two microalgae species, *Cyanobacterium* sp. (AB1166) and *Arthrospira platensis* (AB2293), studied by Algenol are considered in our model. Different elemental and biomass compositions are applied for each target species referred from Algenol's work and summarized in Table S1 of Supplementary material [13]. The differences in productivity between the two species are discussed

Table 1. Differences in the parameters and assumptions between ORP and PBR [13,20,21]

Category	ORP	PBR
Biorefinery spatial dimensions		
Cultivation area	6,000 acre	2,000 acre
Total size	8,974 acre	3,915 acre
Width	33,041 ft	21,611 ft
Length	9,460 ft	6,462 ft
Cultivation facility costs (based on 10 and 32 g/m ² /day average productivity for ORP and PBR)		
CAPEX	713 MM\$	506 MM\$
Variable OPEX (\$/ton AFDW)	\$211	\$341
Fixed OPEX (\$/ton AFDW)	\$72	\$54
Other parameters		
Water evaporation (ratio)	1	0.035
Blowdown (ratio)	1	0.044
CO ₂ utilization efficiency	50%	90%
Areal biomass productivity (ratio)	1	~3.0 (species dependent)

**Fig. 3. Schematic description of the GIS analysis.**

in a later section.

2-2. GIS Analyses - Biomass Productivity Estimation and Candidate Location Selection

In this stage, GIS is applied to consider various geographical features in the supply chain design. The GIS analysis provides input data and parameters for the mathematical optimization model. For instance, the model uses location information and features of the supply chain components (resource sources, biorefinery candidate locations, and demand stations) as input variables and parameters. The productivity of microalgae biomass is utilized to screen for

high-productivity biorefinery candidates and to define the maximum biofuel potential in each candidate. Therefore, GIS analyses are conducted as depicted in Fig. 3 using the ArcGIS Pro software with three classes of GIS data: land, resources, and climate. The GIS analyses involve two steps: biomass productivity estimation and screening of the candidate locations for biorefinery. In the following, the detailed procedures for each step of the GIS analyses are discussed.

2-2-1. Biomass Productivity Estimation

Daily areal biomass productivities of target species in an ORP

and a PBR are estimated by the mathematical model developed by Algenol. The model is developed to estimate the productivity of AB1166 and AB2293 at semi-continuous operation in a VIPER 3.4 PBR. The model parameters were fitted using the data obtained from the outdoor cultivation experiment done in May to June 2018 using 324L VIPER PBRs installed in Fort Myers U.S. [13]. After the fitting, the model was validated using the annual productivity data and the result showed that the model prediction closely tracked the biomass productivity data of pilot plants. A detailed explanation of the model can be found in the Supplementary material.

Based on the model, the biomass productivity map of each target region is obtained by a similar procedure as the global suitability analysis, except using the daily weather data of 20 years from January 1st of 1995 to December 31th of 2015 [19]. The 20-year average daily productivity is calculated at every point in the grid and, based on them, seasonal average productivity is computed. The following screening processes and cultivation parameter calculations are performed based on the seasonal average productivity.

2-2-2. Candidate Location Selection

The procedure for the selection of candidate locations can be summarized as having three stages as drawn in Fig. 3. Each stage requires the respective GIS datasets shown in the grey box to generate the results. Since the objective of this study is to compare target regions, the same global GIS datasets should be used for a fair comparison. The GIS data used in the study are summarized in Table 2. First, the available land is screened using a method similar to the global land suitability evaluation, but this step is performed twice while applying the land slope restriction assumptions as 2% and 5% upper limits for constructing ORPs and PBRs, respectively. These assumptions are based on the values used in the previous GIS-based land screening studies for microalgae-based biorefinery [22,23]. After the screening, water bodies such as rivers and lakes are removed from the available land layers for ORPs and PBRs, respectively.

Then, each available land layer is split as unit cells which are sized according to the spatial dimensions of an ORP and a PBR-based facility defined in Table 1. The raw candidates are defined as

the unit cells with over 95% of the cell area available. For example, ORP raw candidates are selected as those unit cells of which available lands exceed 6817 acres in a total cell area of 7176 acres.

Since the model covers a wide region, the procedure results in a high number of raw candidates and makes the optimization computationally intractable. Therefore, the candidate locations are further screened by applying the land, resource, and biomass productivity constraints, as shown in Fig. 3. First, the raw candidates intersected with urban, protected areas, and transportation infrastructures such as airports, highways, and railways are removed from the candidate sets since they may render the construction infeasible. Then, biomass productivity is calculated for each candidate location to select those locations with a productivity value larger than the mean value. After that, the distances from the resource sources are measured and only those locations situated closer than 100 km from both the CO₂ and water sources are retained as candidate locations. If more than 100 locations exist after the screening steps, the top 100 locations are selected based on the productivity values for ORPs and PBRs, respectively. A more detailed description and graphical representation of the procedure for finding candidate locations can be found in Kang et al. [10].

2-2-3. Potential Pipeline Route Design

CO₂ and water for microalgae cultivation are assumed to be transported using pipelines from their sources. Since the construction costs of the pipelines are dependent on the geographical features of the areas they pass through, straight paths are usually not the cost-optimal routes between the resource sources and the biorefinery candidates. Therefore, prior to the supply chain design, the pipeline routes should be designed between each set of the resource sources and the candidates under the cost minimization objective. In this study, we used the least cost path method to design the routes using the weighted-cost surface as an input. The cost surface is 300 m×300 m raster grids generated by integrating the contributions of each geographical feature on the pipeline construction cost. For example, if there are no geographical obstacles in the unit cell, then the construction cost of a pipeline passing the cell is assumed as '1' which is the base case. Relative weights are added

Table 2. Summary of the global GIS data applied in the GIS analysis

Data	Description	Reference
Land data		
Digital elevation map (DEM)	CGIAR-CSI 250 m global data	[17]
Land cover	ESA-CCI 300 m global data	[16]
Wet area	Global Surface Water Explorer	[24]
Urban area	Natural Earth, 1 : 10 m Urban area polygon data	[25]
Road	Global roads open access data set (GROADS)	[26]
Railway	Natural Earth, 1 : 10 m Railway polyline data	[27]
Protected area	World Database on Protected Areas	[28]
Resource data		
Thermal power plant	World Resources Institutes, Global Database Of Power Plants	[29]
Freshwater source	The Global Reservoir and Dam Database (GRanD)v1.3	[30]
Seawater	Natural Earth, 1 : 10 m Coastline	[31]
Weather data (sunlight, air temperature)	NASA POWER database	[19]

for each cell according to the existence and the attributes of each geographical feature in the cell. The raster layers used in the study and the corresponding values of the weights are referred from a CO₂ pipeline route design case study done by MIT [32]. By summarizing all the weight values assigned, the construction cost multiplier for each cell area is calculated.

2-3. Mathematical Optimization Model

The mathematical optimization model from the previous study is modified to accommodate the adjustments in the supply chain design as described in section 3.2. The sets, variables, and parameters are arranged in the Nomenclature section.

The major model modifications can be summarized as follows:

- Pipeline constructions for resource transportations are considered as binary variables
- The objective function is defined as the minimization of biofuel supply unit costs - total costs divided by total biofuel supplies
- The demand of the supply chain is defined as gasoline gallon equivalents of total biofuel supplies - biodiesel, naphtha, and bioethanol

- Strategic decisions (binary variables) are defined as yearly decisions (t_1) and tactical decisions (continuous variables) are defined as seasonal decisions (t_2) to reduce the number of decisions variables
- An inexact parametric algorithm based on Newton's method is applied to solve the problem that handles the fractional term in the objective function

The detailed expressions and explanation of the mathematical model as well as the formulation and the solution strategy of the optimization are summarized in Supplementary Material.

RESULTS & DISCUSSION

1. Case Studies

A three-stage framework was applied to design a microalgae-based biofuel supply chain in each region selected by the global land suitability analysis - Northern Territory of Australia and La Guajira of Colombia, and Texas of U.S. The analysis results are shown in Supplementary Material. The design assumptions are applied equally in each case study for a fair comparison between

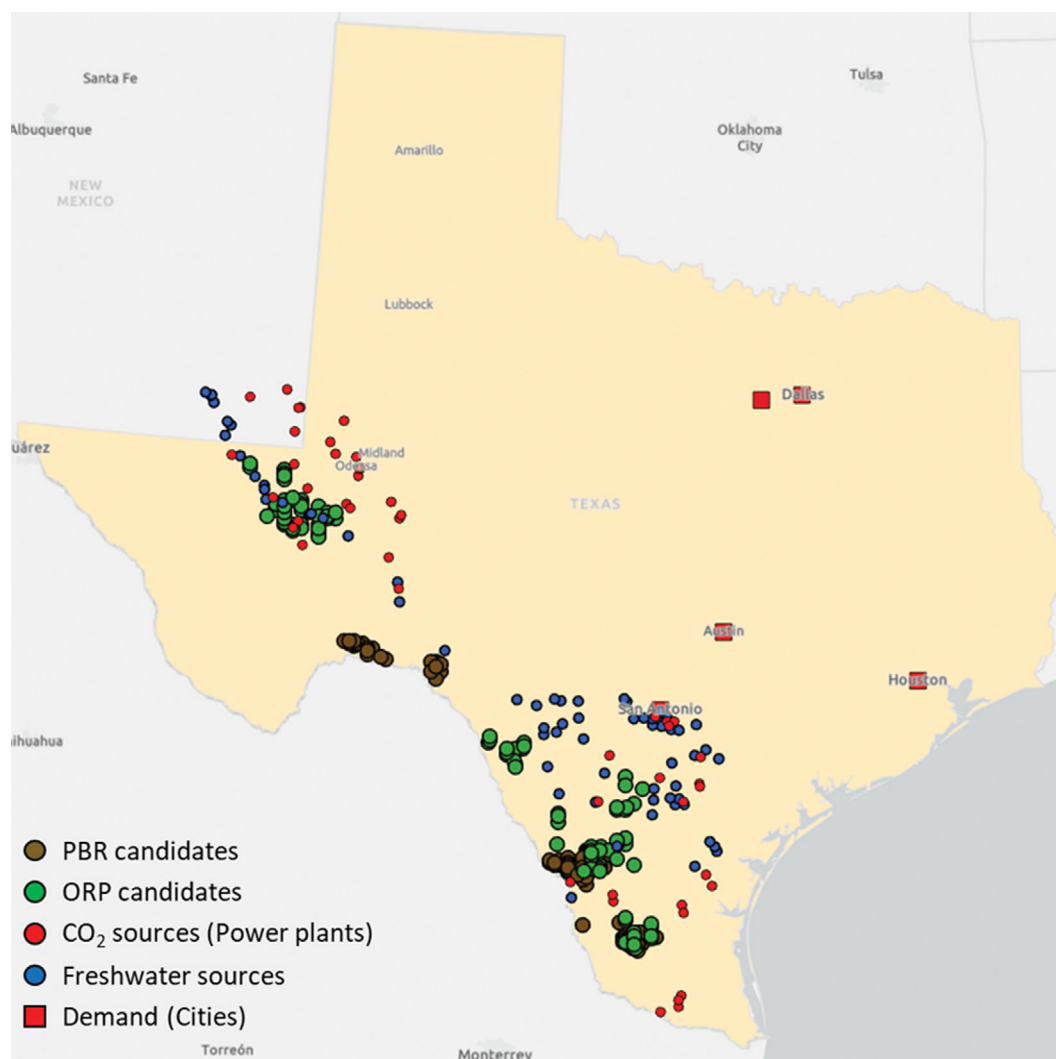


Fig. 4. Candidate locations and resource sources in Texas, U.S.

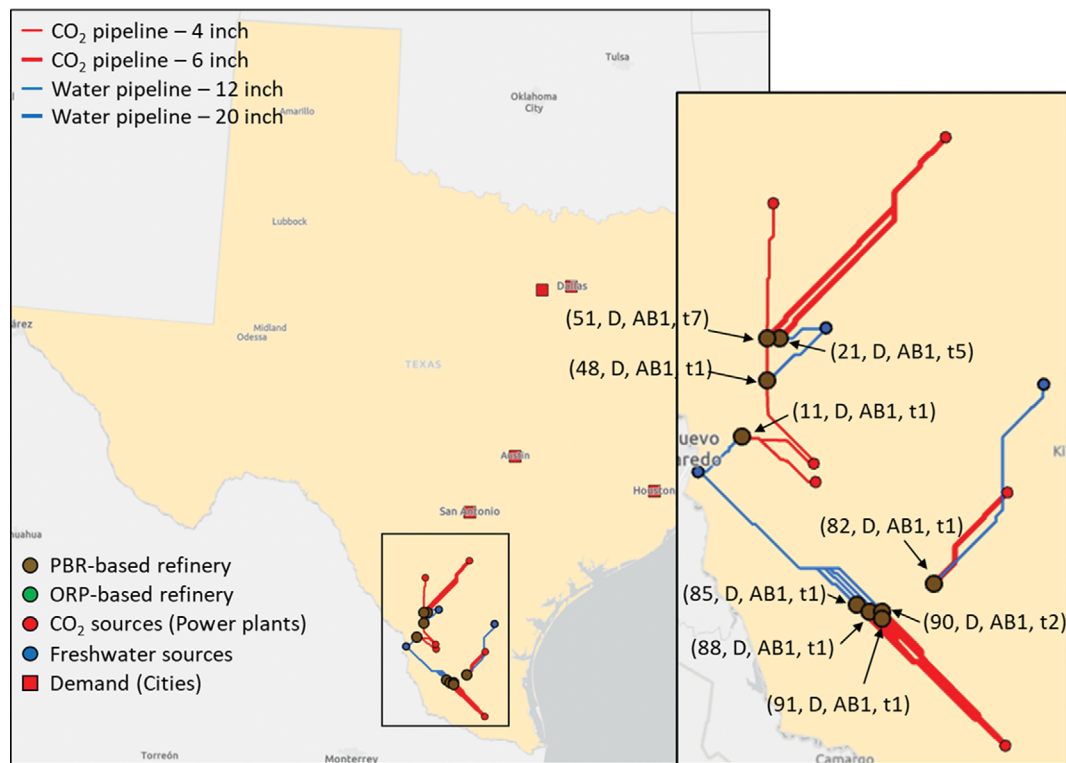


Fig. 5. Designed supply chain configuration in Texas. The information in brackets is the location number, processing pathway (D - direct HTL, P - protein extraction, and F - fermentation), species (AB1 - AB1156, Arth - AB2293), and construction time in order.

those regions, and most of the assumptions from the previous study [10] are kept. The modifications and the added assumptions are as follows:

- The planning horizon for the supply chain is assumed to be seven years, the binary decisions are made for seven periods, while the continuous variable decisions are made for 28 periods.
- The total minimum demands for biofuel in all the case study areas are assumed to be the same as the sum of the demands used in the Texas case study performed in the previous study [10]
- 70% of nitrogen and phosphorous inputs are available to recycle
- The yield of biocrude from HTL is assumed as 40 wt% for all species and processing pathways
- Products are transported to a demand city or a port for transportation of the products

In this section, the case study performed in each target region is explained in detail.

1-1. Texas, U.S.

The GIS analyses screened 100 candidate locations each for PBR- and ORP-based biorefineries, and 52 CO₂ sources, and 72 freshwater sources within 100 km from the candidates as shown in Fig. 4. Since the number of candidate locations screened using the resource and transportation criteria are larger than 100 for both ORP and PBR, only the top 100 locations are chosen as the final candidates. The candidates are congregated in the south and west sides of Texas and thus only the resource sources near the candidates are considered after screening the sources in the whole Texas state to reduce the computational burden of the model. Based on

the candidates screened, the mathematical optimization model is solved using the CPLEX solver of GAMS 25.1.3 using a desktop equipped with i9-9990K CPU @ 3.60 GHz and 64.0 GB RAM.

The designed supply chain is shown in Fig. 5. A total of nine PBR-based biorefineries are constructed and all the biorefineries selected the direct HTL processing pathway and the AB1166 species. In the starting period, the supply chain includes six biorefineries, with additional biorefinery constructed to satisfy the increasing demand in year 2, 5, and 7 at location 90, 21, and 51, respectively. All the biorefineries selected AB1166 as a cultivation species due to its better economics than AB2293 seen in all the processing pathways. This is mainly due to the higher biomass productivity of AB1166 compared to AB2293, which is predicted to be about 10% higher by the productivity estimation model. The biorefineries selected not only the same species but also the same biorefinery design. PBRs dominated over ORPs in the cultivation technology selection due to their lower capital costs and resource requirements compared to ORPs, in spite of their high operating costs. Then, among the byproduct processing pathways, all the biorefineries selected the direct HTL processing pathway without producing any byproduct. Although the species used in this study have high protein content, the price of the protein byproduct targeting the substitution of soybean meal (\$1,000/ton_{protein}) is not high enough to render a selection of the protein extraction pathway. The fermentation pathway is not selected since the maximum biofuel production potential of a biorefinery is slightly lower than the direct HTL pathway (by about 2%) while requiring additional processes. In CO₂ transportation, two diameters of CO₂ pipelines are selected: 4

Table 3. Cost summary of the case studies, TX - Texas, NT - Northern Territory, and LG - La Guajira

Components	Value (MM \$/yr)		
	TX, U.S.	NT, Australia	LG, Colombia
CO ₂ transportation cost	192.0	85.9	252.1
Freshwater transportation cost	107.6	33.7	146.5
Biodiesel transportation cost	25.9	13.7	9.0
Naphtha transportation cost	8.3	2.7	1.8
Protein transportation cost	-	-	-
Bioethanol transportation cost	-	-	-
Total transportation cost (C^{trans})	333.8	140.0	409.4
Transportation cost per unit (\$/GGE)	0.83	0.47	1.25
CO₂ capture cost	351.5	257.7	286.6
Capital cost	3,448.0	2,258.1	2,397.5
Fixed operating cost	238.0	155.6	169.3
Variable operating cost	1682.0	1,045.1	1,196.6
Nutrient cost	160.7	117.8	131.0
Inventory cost	-	-	0.3
Total biorefinery cost ($C^{refinery}$)	5,530.1	3,591.3	3,894.7
Biorefinery cost per unit (\$/GGE)	13.74	12.17	11.86
Revenue from protein (RV)	-	-	-
Total cost ($C^{trans} + C^{refinery} - RV$)	6,216.2	3,985.0	4,590.8
Total biofuels supplied (MM GGE)	402.5	295.1	328.3
Minimum biofuel demand (MM GGE)	294.0	294.0	294.0
Minimum biofuel production cost per unit (\$/GGE) to nearest half dollar.	15.5	13.5	14.0

and 6 inches. The CO₂ requirement of the selected design of biorefinery in the summer season (about 52,000 ton_{CO2}/season) is higher than the maximum capacity of a 4-inch CO₂ pipeline (47,500 ton_{CO2}/season), which leads to the construction of 6-inch pipelines. This leads to an underutilization of the CO₂ pipeline capacity owing to the biomass productivity fluctuations. For instance, the range of average biomass productivity in a year using a PBR with AB1166 species in Texas is 16.4 g DW/day/m² to 40.0 g DW/day/m², meaning the productivity of the winter season is only about 40% of that of the summer season. On the other hand, in water transportation, water pipelines are selected as the minimum diameter option in the model since the water requirements of the PBRs are much lower than the ORPs. Moreover, the water requirement is controlled by the evaporation and blowdown rate of a season, and the fluctuations between seasons are less than the productivity. This leads to better utilization of the pipeline capacity compared to the CO₂.

The cost of the designed supply chain is summarized in Table 3. The total production cost per unit of biofuel produced was \$15.50/GGE in Texas, which is the highest value among the cases in this study. This is mainly due to the low average and high fluctuation of biomass productivity compared to the other two regions. Especially, the productivity fluctuation results in a significant underutilization of the downstream process and the CO₂ pipeline capacity, which in turn leads to both the high biorefinery and transportation cost per unit biofuel. Among the major items of the costs, the biorefinery costs overwhelmed the others, owing to the high capital and operating costs of a biorefinery. This result is similar to the

prior study [10] despite the different economic data and assumptions used, which supports the conclusion that the reduction of the biofuel production cost is the key to the commercialization of microalgae-based biofuel.

1-2. Northern Territory, Australia

The GIS analyses screened 100 PBR-based and 20 ORP-based candidate locations, and five CO₂ sources, and three freshwater sources in Northern Territory (NT), Australia as shown in Fig. 7. In this region, the number of available ORPs is less than 100, so the productivity criterion for further screening was not applied to the ORP candidates. The candidate locations are clustered near Darwin and western border of NT, which shows high biomass productivity values among the raw candidate locations. The year-average biomass productivity of AB1166 in the PBR candidates is 33.9 g/m²/day, and the seasonal productivity value fluctuates from 30.3 g/m²/day to 40.2 g/m²/day. The resource sources are located near the candidates, though the number of locations is fewer than in the Texas case. The demand market of the case study is set as Darwin, Australia as marked by the purple dot in Fig. 6, which would take a role as biofuel terminal for further distribution to other Australian cities or Asian markets. The amount of demand is set as the sum of the demands in the five cities of Texas.

Based on the locations screened, the supply chain is designed as presented in Fig. 7. A total of six PBR-based biorefineries are constructed and all the biorefineries selected the same design as the Texas case - the direct HTL processing pathway, and the AB1166 species. The supply chain includes four biorefineries in the initial

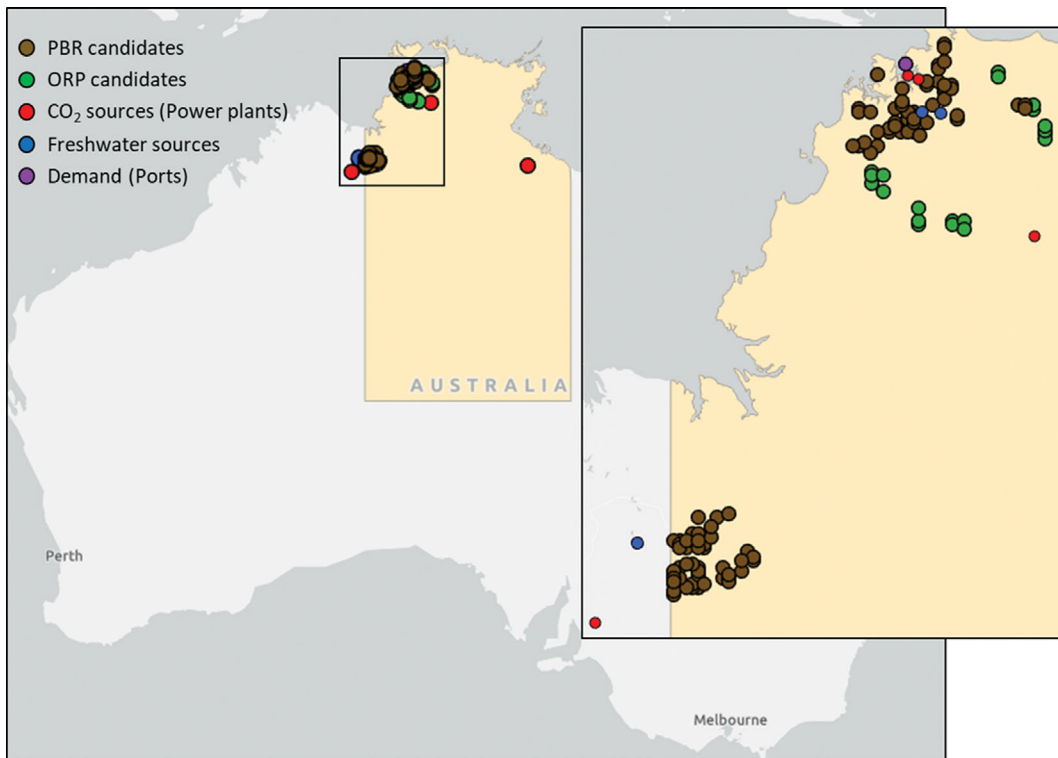


Fig. 6. Screened candidate locations and resource sources in Northern Territory, Australia.

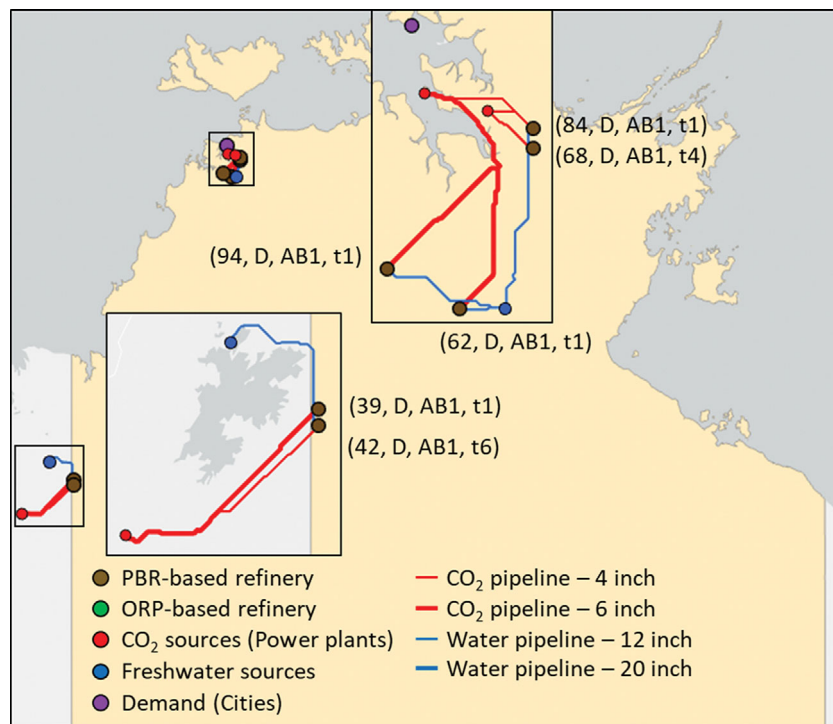


Fig. 7. Designed supply chain in Northern Territory, Australia.

period, and an additional biorefinery is constructed to location 68 and 42 in year 4 and 6, respectively. The supply chain produces biofuel just over the minimum demand, whereas the Texas case produces 37% higher than the minimum demand in order to have

the lowest cost per unit biofuel. This results in a lower number of biorefineries constructed in the supply chain of NT compared to the Texas case. In the resource transportation, the two diameters of CO₂ pipelines used in the Texas case and just a single (minimum)

diameter of water pipelines were selected. Also, similar to the Texas case, the CO₂ requirement in the autumn season (about 54,000 ton_{CO2}/season) is higher than the maximum capacity of a 4-inch CO₂ pipeline. However, the underutilization of each of the capacities is not significant since the productivity fluctuation is lower compared to the Texas case.

The cost of the supply chain of NT is summarized in Table 3. The total production cost per unit biofuel produced resulted in \$13.50/GGE in NT, which is significantly lower than that of the Texas case. This is mainly owing to the higher average and lower fluctuation of the biomass productivity. This is expected as productivity fluctuation results in significant underutilization of the downstream processes and CO₂ pipeline capacity, which in turn gives both high biorefinery and transportation cost per unit biofuel. These can be confirmed by the lower unit biorefinery costs and unit transportation costs in NT compared to Texas while using the same biorefinery design and similar pipeline length and diameter.

1-3. La Guajira, Colombia

The GIS analyses are also performed for La Guajira (LG), Colombia to screen the biorefinery candidate locations, resource sources, and distance data. The analyses resulted in 57 PBR-based and two ORP-based candidate locations, and one CO₂ and freshwater source, each as shown in Fig. 8. In this region, the number of candidates and resource sources is much less than in the other two case studies. This makes the maximum amount of biofuel production to be restricted by resource availability. Moreover, the distances between the resource sources and candidates are farther than in the other two cases, which may result in higher transportation cost. The year-average biomass productivity of the AB1166 species in the PBR at the candidate locations is 32.8 g/m²/day, and the seasonal average productivity varies between 30.5 g/m²/day to

35.3 g/m²/day. The average is lower than in Australia, while the variation is the smallest among the case study areas. The demand market of the case study is set as Puerto Bolivar, which is the largest port in Colombia, as marked by the purple dot in Fig. 9. The amount of demand is kept the same as in the prior two case studies.

The supply chain in LG is designed as Fig. 9. Six PBR-based biorefineries using the same design as in the prior two cases are constructed. The initial supply chain includes four biorefineries, and an additional biorefinery is constructed each to location 33 and 31 in year 2 and 5, respectively. The biofuel supply for the lowest unit production cost is about 12% higher than the minimum demand, which is slightly higher compared to the Australia case. In resource transportation, only the smallest diameter is used for both the CO₂ pipelines and water pipelines, owing to the lower biomass productivity variation between the seasons. The maximum CO₂ requirement of the biorefinery is 46,400 ton_{CO2}/season, which is less than the maximum capacity of a 4-inch pipeline.

The cost summary of LG is presented in Table 3. The total production cost per unit of biofuel is \$14.00/GGE in LG. Although LG showed the lowest unit biorefinery cost among the case studies, the unit total production cost is higher than in NT owing to the high transportation cost. The lowest biorefinery cost achieved in LG owes to the lowest fluctuation of biomass productivity, though the average biomass productivity is slightly lower than in NT. The low variation of the productivity allows for efficient utilization of the biorefinery processing capacity year round. However, all the distances between the resource sources and the biorefinery are over 140 km, which are much farther than in the other two cases. This makes the unit transportation cost to be almost three times that of NT, even though the CO₂ pipelines are constructed only with the smallest diameter.

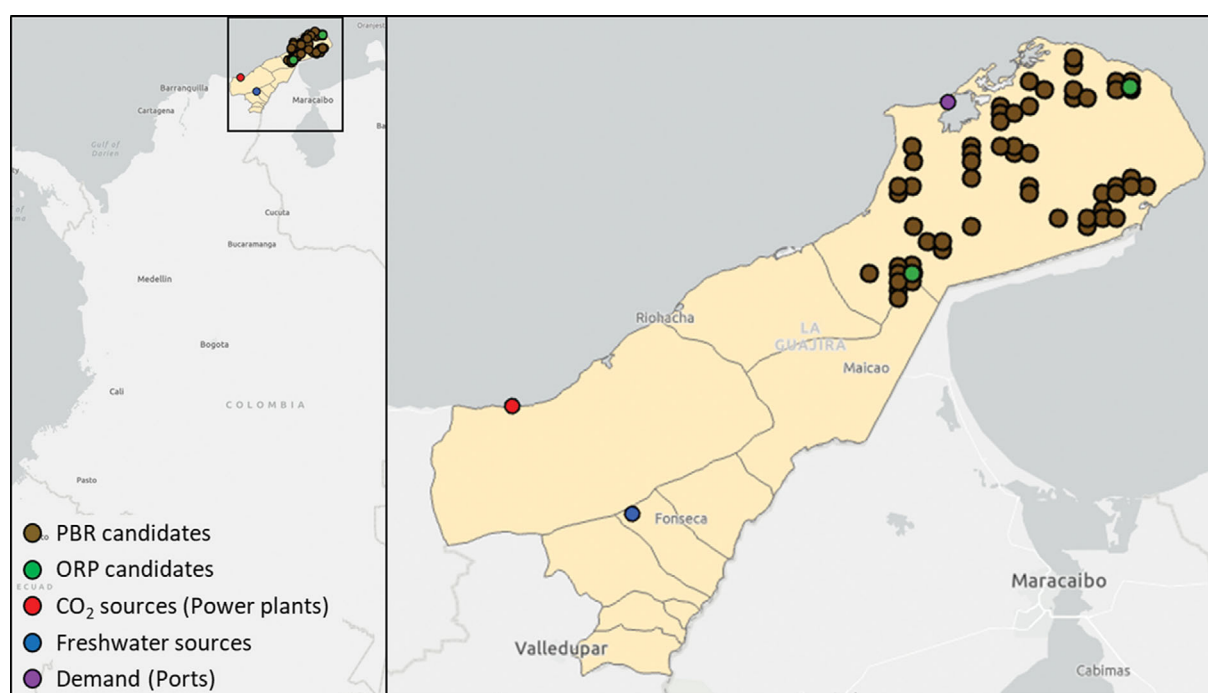


Fig. 8. Screened candidate locations and resource sources in La Guajira, Colombia.

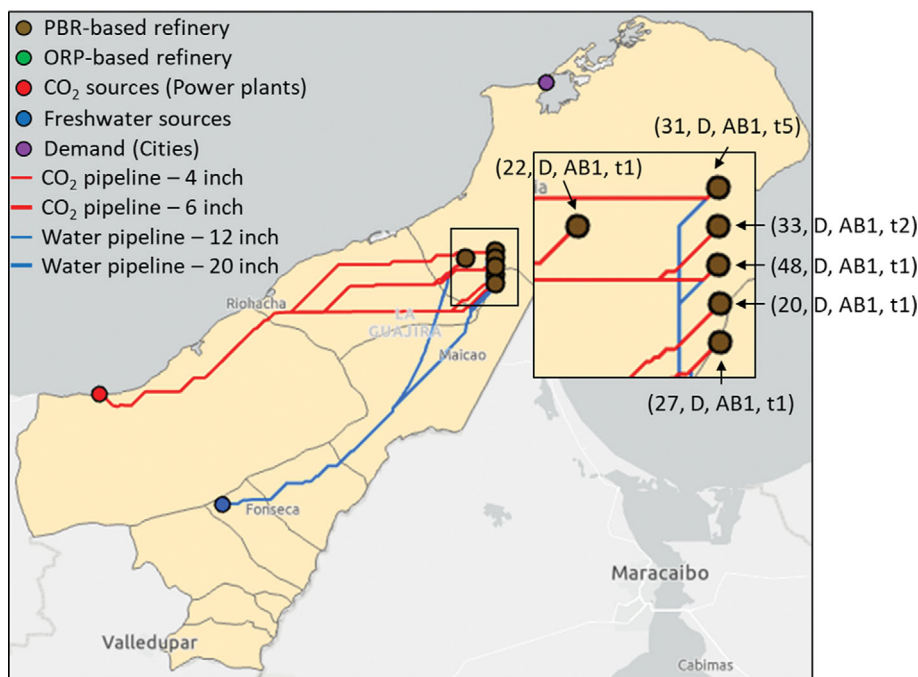


Fig. 9. Designed supply chain in La Guajira, Colombia.

2. Discussion

By applying the three-stage design framework in each region, the optimal supply chain is designed under the minimization of unit biofuel production cost. In all the supply chains, the same biorefinery design is applied – PBR-based, direct HTL, and AB1166 species. This shows the effect of geographical characteristics is minimal on the economic rank of the biorefinery designs applied in the study. The species applied in this study have similar characteristics, including biomass composition, water type, biofuel yield, and optimal cultivation temperature. Thus, only AB1166 is selected owing to its higher biomass productivity in all the case study regions. The species selection can vary when species having different characteristics with comparable biomass productivity are applied in the model. For instance, if saline water species have a similar level of biofuel productivity with AB1166 considered in the model, it may show better economic performance than AB1166 in the Colombia case since the freshwater source and biorefinery candidate locations are widely separated and the resource capacity is limited. Therefore, additional studies should be done to develop the process data of promising microalgae species having different characteristics to investigate whether the optimal species can differ according to the geographical features. For processing pathway differentiation, by-product pathways would be selected if high-value byproducts with better economics and enough market demand exist, despite the sacrifice in the biofuel productivity and the additional capital and operating costs. For example, if microalgae-based proteins are used as a substitutional protein source over fish meals, their price can be set at over \$2/kg [33].

As revealed in the GIS analyses, some regions, such as Colombia, lack resource sources and even the existing ones may not be close to the biorefinery candidate locations. In such regions, the

biofuel demand may not be met due to the lack of resources and require unrealistically long pipeline transportation. Thus, alternate resource supply methods should be considered to overcome this problem. As mentioned, using saline water species can switch the water supply from freshwater to saline water, including groundwater and seawater. This can relax the supply capacity constraints and may reduce the transportation distances. For example, biorefinery candidates in Colombia can be located near the seashore, which can reduce transportation costs significantly. On the other hand, an alternative CO₂ supply can be considered, such as by employing a direct air capture technology, to alleviate the resource transportation issues. To pursue this, we examined the effect of direct air capture cost on the supply chain configuration and the results are shown in the next section.

Compared with the supply chain designed in the previous study, which was for the same location (Texas) and had the same basic biofuel production trend as the current design, the designed supply chain in the current study showed almost twice higher unit production cost (\$7.92/gal_{biodiesel}) [10]. In the previous study, we assumed a 25 g/m²/day annual average productivity value for the ORP-based cultivation, which was a projection target value from an NREL report and had not been experimentally demonstrated. On the other hand, the productivity estimation model developed by the use of pilot-scale cultivation data resulted in a significantly lower annual average biomass productivity value of 9.4 g/m²/day for the ORP-based cultivation in Texas. This productivity gap is responsible for the vastly different unit production costs of the designed supply chains. This reinforces the conclusion that algal productivity is the overriding driver of the economics of biofuels and that there is a gap between the state-of-the-art and the future projected productivity values.

SCENARIO STUDY

1. Direct Air Capture (DAC)

Since the supply of CO₂ is revealed to be a major active constraint in the supply chain design, a direct air capture (DAC) option is considered as an alternative for CO₂ supply. One technological implementation of DAC can capture industrial-scale quantities of CO₂ from an atmosphere using an aqueous KOH sorbent coupled to a calcium caustic recovery loop [34,35]. The DAC facility is integrated into biorefineries to allow for a stable CO₂ supply to the biorefineries without the transportation cost. Therefore, there is a trade-off in each biorefinery between the DAC cost and CO₂ transportation cost by pipeline, which would be dependent on the distances between the CO₂ sources and the biorefinery.

In this study, we applied the aqueous DAC system developed by Carbon Engineering, which designed the 1Mt-CO₂/year industrial-scale facility [34]. The company estimated the levelized capture cost per ton CO₂ and provided a range of \$94 to \$232/ton-CO₂ in the reference. We assumed three cost levels of direct air capture, \$150/ton, \$100/ton, and \$50/ton, reflecting an aggressive cost reduction program. These are referred to as scenarios 1, 2, and 3, respectively, in the scenario study to identify how the supply chain configuration, and costs are changed according to the cost level of DAC. The mathematical model is solved again for each scenario with the additional constraint and the modified objective function to consider DAC, which are summarized in Supplementary Material.

We present the scenario study results in Australia as a represen-

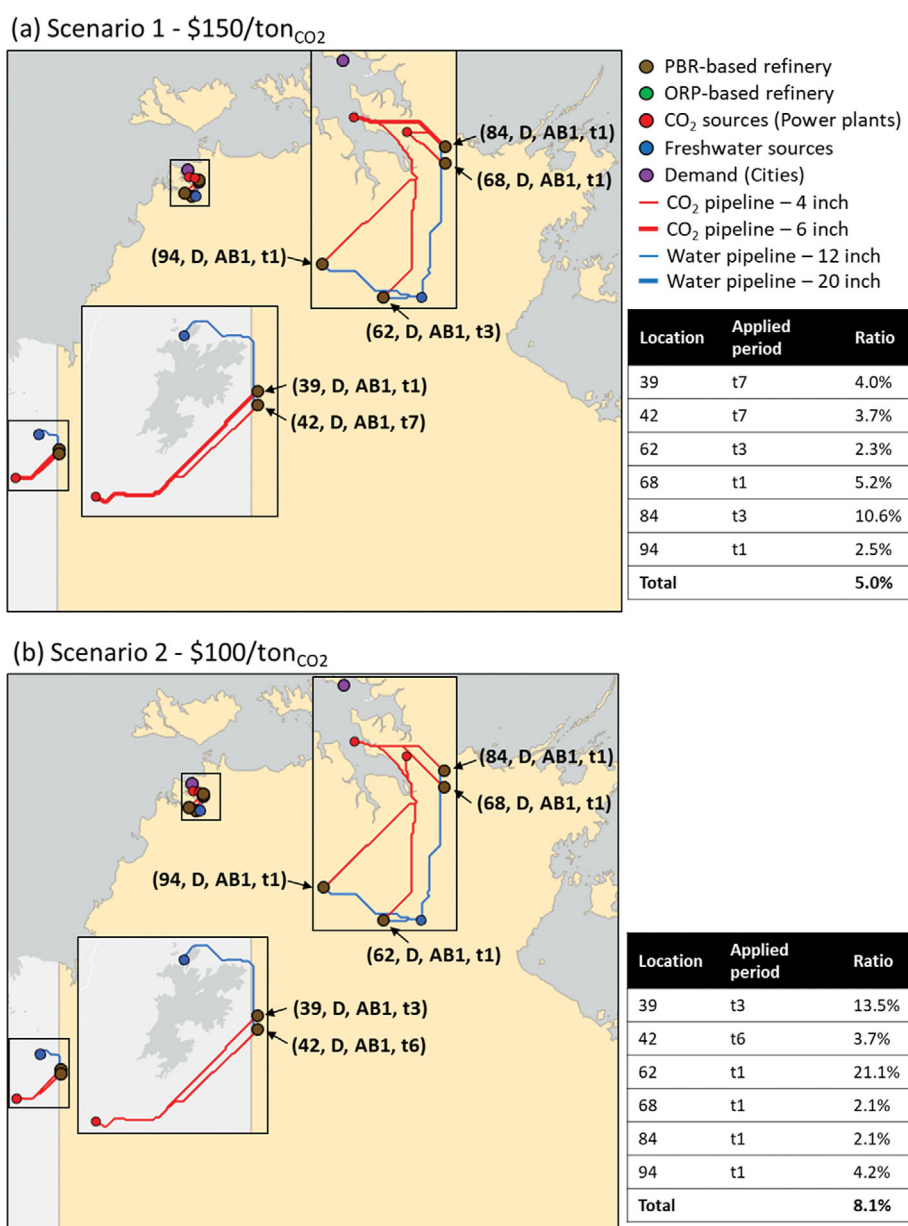


Fig. 10. Direct air capture scenario study results in Australia (a) \$150/ton_{CO2}, (b) \$100/ton_{CO2}, and (c) \$50/ton_{CO2}, the table shows the period DAC applied and the ratio of CO₂ supplied using DAC against total CO₂ supplied to each biorefinery.

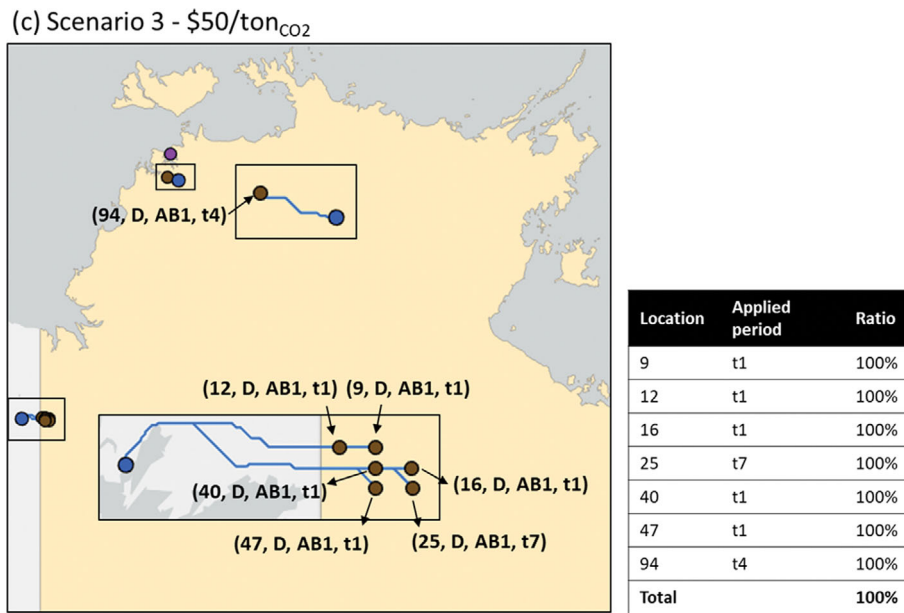


Fig. 10. Continued.

tative case. The results of the other case study areas are summarized in Supplementary Material. The supply chain configurations of the three scenarios are represented in Fig. 10. The table placed on the right side of the figure summarizes the ratio of CO₂ supplied by DAC against the total CO₂ supplied to each biorefinery. As the DAC cost decreases, more CO₂ is supplied to biorefineries through DAC as expected. In scenario 1, DAC supplies 5.0% of the total CO₂ supply, while in the \$100/ton_{CO2} scenario, 8.1% of CO₂ supply is through the DAC. Between these two scenarios, only the CO₂ pipelines and the construction period of the biorefineries are slightly altered in the configuration, while the number, process design, and locations of biorefineries remain unchanged. In scenario 1, one of the four biorefineries in the northern area (location 62) is constructed in year 3, while all the biorefineries are constructed in the starting period in scenario 2. In scenario 1, the pipeline supply is preferred rather than the DAC due to the high cost, and only a small amount of CO₂ is supplied using DAC in two of the biorefineries in the starting period. Thus, the limited CO₂ source capacity allows only three biorefineries (location 68, 84, and 94) to be constructed in the northern area in the starting

period. In year 3, an additional biorefinery and pipeline are constructed on location 62 to meet the biofuel demand increase, while in location 84, the CO₂ supply from the distant sources is decreased and is replaced by DAC. On the other hand, in scenario 2, the biorefineries prefer DAC more than in scenario 1 as the cost is reduced, which results in all four biorefineries in the northern area being constructed from the start. In scenario 3, the CO₂ supply is entirely done by DAC and no CO₂ pipelines are constructed. This frees the supply chain from the CO₂ supply constraints and results in a complete change of the supply chain configuration. The result shows that biorefineries are constructed in locations that have the highest productivity levels and near freshwater sources.

The cost summaries of the DAC scenario case studies are presented in Table 4. The total cost per unit decreases 2.7%, 3.2%, and 5.2% from the base case in scenarios 1, 2, and 3, respectively. This decrease originates from the decrease in the CO₂ supply cost per unit product GGE, which is \$1.22/GGE for scenario 1 and \$0.97/GGE for scenario 3. Also noteworthy is the increase in the amount of biofuel production as the DAC cost decreases. As the CO₂ supply constraint is relaxed, the biorefinery locations with

Table 4. The cost summary of DAC scenarios

Components (MM\$)	Scenario 1	Scenario 2	Scenario 3
CO ₂ transportation cost	76.3	69.9	-
Total transportation cost (C^{trans})	126.3	118.4	96.3
CO ₂ capture cost (C^{CO2CAP})	257.0	255.8	-
Direct air capture cost (C^{DAC})	45.5	50.0	361.3
CO₂ supply cost ($C^{trans, CO2} + C^{CO2cap} + C^{DAC}$) per unit (\$/GGE)	1.22	1.18	0.97
Total cost ($C^{trans} + C^{refinery} - RV$)	4,070.2	4,166.0	4,764.2
Total biofuels supplied (MM GGE)	310.0	318.7	372.3
Minimum biofuel demand (MM GGE)	294.0	294.0	294.0
Minimum biofuel cost per unit (\$/GGE)	13.13	13.07	12.80

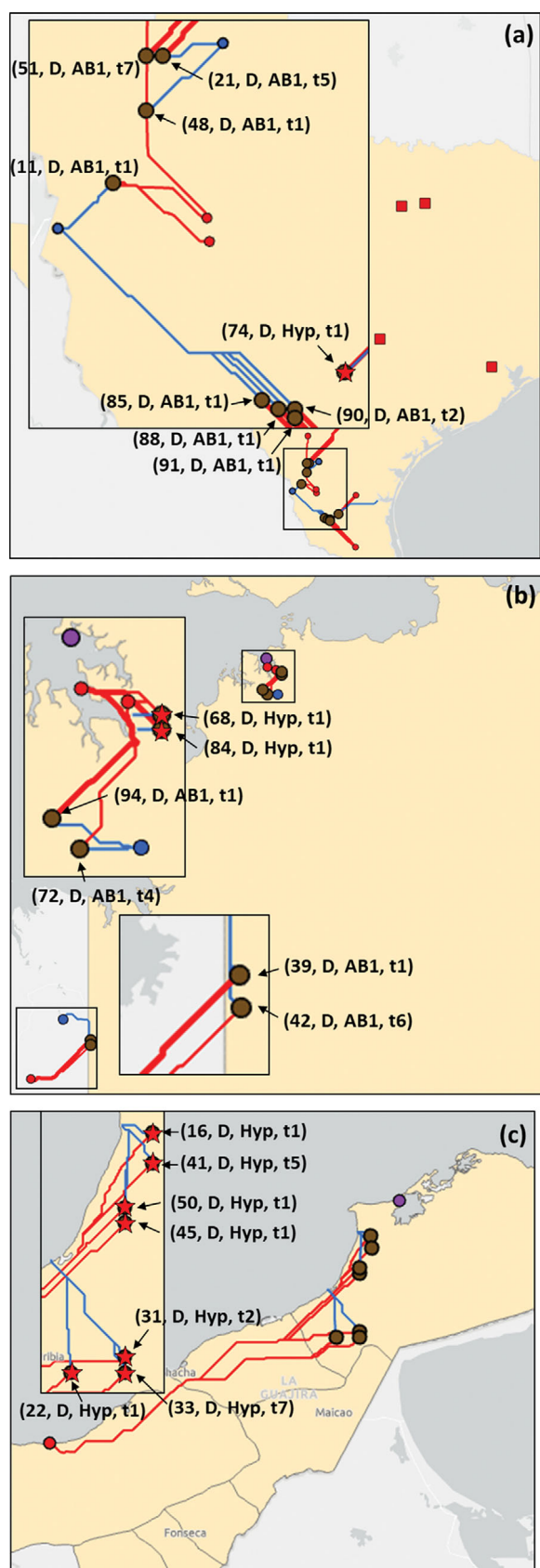


Fig. 11. Hypothetical saline water species scenario results in (a) Texas, (b) Northern Territory, and (c) La Guajira, red-colored stars indicate the biorefinery using hypothetical species.

high productivity but lacking CO_2 supplies or with locations far from the source can produce biofuel at a low cost. In summary, DAC is a promising alternative CO_2 supply method for microalgae-based biorefinery for certain locations.

2. Hypothetical Saline Water Species

As mentioned in the Discussion, using saline water species that have comparable biofuel productivity with AB1166 may show better economics in the supply chain by easing the water supply constraints. In this scenario study, we compared AB1166 with a hypothetical saline water species that has the same characteristics and productivity as AB1166 but uses different water quality, in order to investigate whether the use of such a species affects the supply chain design and cost. To consider the saline water species option in the model, some original constraints are modified and additional constraints and cost items are added. The constraints and cost items are explained in Supplementary Material.

Using the modified model, the hypothetical species scenarios are tested in three target regions and the resulting supply chains are shown in Fig. 11. In all three regions, the hypothetical species is selected in the biorefinery design, one in Texas, two in NT, and all seven biorefineries in LG. Since all species characteristics except water type are assumed to be the same, the selection of hypothetical species is governed by water supply costs. In Texas, the candidate locations are far from the sea, and using saline water species cannot significantly save on water supply costs, as locations 85, 88, 90, and 91 have long supply distances. Therefore, only one biorefinery on location 82 in the base case design is replaced by a biorefinery on location 74 that uses the hypothetical species. In NT, the two biorefineries, locations 68 and 84, located near the seashore select the saline water species. Compared with the base case design, there are no changes in the design and locations in the other biorefineries except the biorefinery on location 62 moves to location 72. Lastly in LG, the supply chain design is changed as the saline water species option is applied. Since the distances between the freshwater source and the candidate locations are long in Colombia, all the biorefineries selected the hypothetical species and were constructed near the seashore to reduce the water supply costs.

The cost summaries of the scenario studies in each region are presented in Table 5. The unit water supply costs of the supply chain are reduced in all the target regions. However, as the supply distances are decreased only marginally in Texas and NT, their cost reduction is not significant. In contrast, in LG, the water supply cost is reduced by 82% from the base case as all the biorefineries are affected by the application of the hypothetical species. While we applied the same biomass characteristics with AB1166 for the hypothetical species, the species characteristics will differ in a real case. The literature reported that saline water species have higher lipid content compared to freshwater species due to their saltwater stresses [36,37]. This implies a higher potential of biofuel yield for saline water species. However, no data is available on whether the growth rates of saline species in PBRs are similar to those of freshwater species, and this is the most significant factor in the cost. Through the scenario study, we can conclude that the benefits from applying saline water species are different according to the geographical characteristics in each region, and the consideration of saline water species can be a promising option if its biofuel yields

Table 5. The cost summary of hypothetical saline water species scenarios

Components (MM\$)	TX, U.S.	NT, Australia	LG, Colombia
Freshwater transportation cost	87.6	22.9	-
Seawater transportation cost	17.5	3.6	27.2
Total transportation cost (C^{trans})	332.0	125.9	313.5
Water supply cost per unit of base case (\$/GGE)	0.27	0.11	0.45
Water supply cost per unit (\$/GGE)	0.26	0.09	0.08
Total cost ($C^{trans} + C^{refinery} - RV$)	6,216.2	3,977.4	4,619.6
Total biofuels supplied (MM GGE)	402.6	295.0	337.7
Minimum biofuel demand (MM GGE)	294.0	294.0	294.0
Minimum biofuel cost per unit (\$/GGE)	15.4	13.5	13.7

are similar to freshwater species.

CONCLUSION

Microalgae-based biofuel supply chains were designed in three different regions, considering the geographic conditions of each region, including weather, resource, and land area. The target regions were selected through global suitability analysis under land availability and biomass productivity criteria, which are the basic requirements for an industrial scale microalgae-based biofuel production. The design framework developed in a prior study was enhanced to consider the additional cultivation technology of photobioreactor and perform gasoline gallon equivalent unit-based optimization. Moreover, the biomass productivity estimation model and the process data generated from the pilot-scale facility operated by Algenol were applied to consider more realistic designs and costs under the current technology level. The formulated mathematical optimization problem was mixed-integer fractional programming, which cannot be solved by off-the-shelf nonlinear solvers; hence, a tailored solving algorithm was applied to solve the problem.

Case studies were performed in three selected regions – the State of Texas, the U.S., Northern Territory of Australia (NT), and La Guajira, Colombia (LG) – and cost-optimal supply chains were designed. According to the geographical conditions of each area, different supply chain designs and costs result. The total unit production cost was calculated as \$15.4, \$13.5, and \$14.0/GGE in Texas, NT, and LG, respectively. The low average and high fluctuations of biomass productivity in Texas resulted in the highest unit production cost. Between NT and LG, LG showed lower biorefinery costs due to the lower productivity fluctuations, though average biomass productivity is slightly lower compared to NT. The low productivity fluctuation prevented an underutilization of the downstream processes and pipeline capacity. However, long distances between resource sources and biorefinery locations in the LG region brought higher transportation costs, which led to higher overall unit production costs. Thus, alternative resource supply scenarios of direct air capture and the adoption of a saline water species were implemented to test the effect of relaxing the resource supply constraints. These scenario studies showed that, by relaxing resource supply constraints, the economics can be improved and different designs are generated.

Using the developed framework, we can identify regions with

high potential for microalgae-based biofuel under the land availability and productivity criteria, and propose cost-optimal supply chain designs with candidate locations and resource sources screened by GIS-based analyses. While we performed three case studies in this study, the proposed framework can design algae system supply chains in any global region, provided GIS data is available. The framework can provide a cost comparison of different processing pathways and microalgae species integrating geographical features and constraints.

ACKNOWLEDGEMENTS

This work was supported by the Carbon-to-X (C2X) R&D project (project no. 2020M3H7A1096361) sponsored by the National Research Foundation (NRF) of the Ministry of Science and ICT.

SUPPORTING INFORMATION

Additional information as noted in the text. This information is available via the Internet at <http://www.springer.com/chemistry/journal/11814>.

REFERENCES

1. Z. Navas-Anguita, D. García-Gusano and D. Iribarren, *Renew. Sust. Energ. Rev.*, **112**, 11 (2019).
2. World Energy Outlook 2019, International Energy Agency (2019).
3. Z. Zhang, L. Lohr, C. Escalante and M. Wetzstein, *Energy Policy*, **38**, 445 (2010).
4. S. Tayari, R. Abedi and A. Rahi, *Renew. Energy*, **147**, 1058 (2020).
5. A. Schwab, Bioenergy Technologies Office Multi-Year Program Plan. March 2016, Bioenergy Technologies Office (2016).
6. J. C. Quinn and R. Davis, *Bioresour. Technol.*, **184**, 444 (2015).
7. S. Banerjee and S. Ramaswamy, *Bioresour. Technol. Rep.*, **8**, 100328 (2019).
8. D. F. Correa, H. L. Beyer, H. P. Possingham, S. R. Thomas-Hall and P. M. Schenk, *Glob. Change Biol. Bioenergy*, **11**, 914 (2019).
9. K. G. Nodoshan, R. J. Moraga, S.-J. G. Chen, C. Nguyen, Z. Wang and S. Mohseni, *Ind. Eng. Chem. Res.*, **57**, 6910 (2018).
10. S. Kang, S. Heo, M. J. Realff and J. H. Lee, *Appl. Energy*, **265**, 114773 (2020).
11. S. Mohseni, M. S. Pishvaei and H. Sahebi, *Energy*, **111**, 736 (2016).

12. S. Kang, S. Heo and J. H. Lee, *Ind. Eng. Chem. Res.*, **58**, 944 (2018).
13. R. Chance and P. Roessler, Production of Biocrude in an Advanced Photobioreactor-Based Biorefinery, Algenol Biotech (2020).
14. A. Karemore, Y. Yuan, W. Porubsky and R. Chance, *Biotechnol. Bioeng.*, **117**, 3081 (2020).
15. Z. Zhong and F. You, *Comput. Chem. Eng.*, **61**, 90 (2014).
16. European Space Agency Climate Change Initiative Land Cover <https://www.esa-landcover-cci.org/> (accessed July 2020).
17. CGIAR-CSI SRTM 90m Digital Elevation Database v4.1, <https://cgiarcsi.community/data/srtm-90m-digital-elevation-database-v4-1/> (accessed March 2020).
18. J. Ferrell and V. Sarisky-Reed, National Algal Biofuels Technology Roadmap, U.S. Department of Energy, Office of Energy Efficiency and Renewable Energy, Biomass Program. (2010).
19. NASA Prediction Of Worldwide Energy Resources, <https://power.larc.nasa.gov/data-access-viewer/> (accessed November 2020).
20. J. N. Clippinger and R. E. Davis, Techno-Economic Analysis for the Production of Algal Biomass via Closed Photobioreactors: Future Cost Potential Evaluated Across a Range of Cultivation System Designs, National Renewable Energy Laboratory (2019).
21. Q. Li and C. E. Canter, Greenhouse Gas Emissions, Energy and Water Use of Photobioreactors for Algal Cultivation and Biofuels Production, Argonne National Laboratory (2017).
22. J. C. Quinn, K. B. Catton, S. Johnson and T. H. Bradley, *Bioenergy Res.*, **6**, 591 (2013).
23. E. R. Venteris, R. C. McBride, A. M. Coleman, R. L. Skaggs and M. S. Wigmosta, *Environ. Sci. Technol.*, **48**, 3559 (2014).
24. The European Commission Joint Research Center, Global Surface Water Explorer, <https://global-surface-water.appspot.com/#data> (accessed October 2020).
25. Natural Earth, 1:10m Urban areas, <https://www.naturalearthdata.com/downloads/> (accessed March 2020).
26. NASA Socioeconomic Data and Applications Center, Global Roads Open Access Dataset v1, <https://sedac.ciesin.columbia.edu/data/set/groads-global-roads-open-access-v1> (accessed August 2020).
27. Natural Earth, 1:10m Railroads, <https://www.naturalearthdata.com/downloads/> (accessed March 2020).
28. International Union for Conservation of Nature, The World Database on Protected Areas, <https://www.protectedplanet.net/en/thematic-areas/wdpa> (accessed May 2020).
29. World Resources Institute, Global Power Plant Database, <https://datasets.wri.org/dataset/globalpowerplantdatabase> (accessed October 2020).
30. NASA Socioeconomic Data and Applications Center, Global Reservoir and Dam v1.3, <https://sedac.ciesin.columbia.edu/data/set/grand-v1-dams-rev01> (accessed August 2020).
31. Natural Earth, 1:10m Coastline, <https://www.naturalearthdata.com/downloads/> (accessed March 2020).
32. H. J. Herzog and H. Javedan, Development of a Carbon Management Geographic Information System (GIS) for The United States, Massachusetts Institutes of Technology, Energy Laboratory (2010).
33. R. S. C. Barone, D. Y. Sonoda, E. K. Lorenz and J. E. P. Cyrino, *Sci. Agric.*, **75**, 184 (2018).
34. D. W. Keith, G. Holmes, D. S. Angelo and K. Heidel, *Joule*, **2**, 1573 (2018).
35. H. Azarabadi and K. S. Lackner, *Appl. Energy*, **250**, 959 (2019).
36. H. Alishah Aratboni, N. Rafiei, R. Garcia-Granados, A. Alemzadeh and J. R. Morones-Ramírez, *Microb. Cell Factories*, **18**, 178 (2019).
37. R. S. Gour, V. K. Garlapati and A. Kant, *Curr. Microbiol.*, **77**, 779 (2020).